Scaling of Spontaneous Rotation with Temperature and Plasma Current in Tokamaks

F. I. Parra, M. F. F. Nave, A. A. Schekochihin, C. Giroud, J. S. de Grassie, J. H. F. Severo, P. de Vries, and K.-D. Zastrow

Scaling of spontaneous rotation with temperature and plasma current in tokamaks

F. I. Parra,[1,2,*] M. F. F. Nave,[3,1] A. A. Schekochihin,[1] C. Giroud,[4] J. S. de Grassie,[5]
J. H. F. Severo,[6] P. de Vries,[7] K.-D. Zastrow,[4] and JET-EFDA Contributors [†8]

[1]*Rudolf Peierls Centre for Theoretical Physics, University of Oxford, Oxford OX1 3NP, UK*
[2]*Plasma Science and Fusion Center, Massachusetts Institute of Technology, Cambridge, MA 02139, USA*
[3]*Associação EURATOM/IST, Instituto de Plasmas e Fusão Nuclear,*
Instituto Superior Técnico, Technical University of Lisbon, Portugal
[4]*Euratom/CCFE Fusion Association, Culham Science Centre, Abingdon OX14 3DB, UK*
[5]*General Atomics, P.O. Box 85608, San Diego, California, USA*
[6]*Institute of Physics, University of São Paulo, SP, Brazil*
[7]*FOM Institute for Plasma Physics, Rijnhuizen, Association EURATOM-FOM, Nieuwegein, The Netherlands*
[8]*JET-EFDA, Culham Science Centre, Abingdon, OX14 3DB, UK*
(Dated: January 5, 2012)

Using theoretical arguments, a simple scaling law for the size of the intrinsic rotation observed in tokamaks in the absence of momentum injection is found: the velocity generated in the core of a tokamak must be proportional to the ion temperature difference in the core divided by the plasma current, independent of the size of the device. The constant of proportionality is of the order of $10 \, \mathrm{km} \cdot \mathrm{s}^{-1} \cdot \mathrm{MA} \cdot \mathrm{keV}^{-1}$. When the intrinsic rotation profile is hollow, i.e. it is counter-current in the core of the tokamak and co-current in the edge, the scaling law presented in this Letter fits the data remarkably well for several tokamaks of vastly different size and heated by different mechanisms.

Introduction. Due to their axisymmetry, tokamak plasmas can be made to rotate at high speeds if momentum is injected into them. If the rotation is sufficiently large, large scale magnetohydrodynamic (MHD) instabilities are stabilized [1] and the turbulent transport of energy can be much reduced [2–4]. Unfortunately, ITER [5], the largest magnetic confinement experiment currently being built, is not expected to have effective momentum deposition due to its size and high density. As a result, there has been mounting interest in the intrinsic, or spontaneous, rotation observed in tokamaks without momentum injection [6]. If this intrinsic rotation could be made large, it could be used to prevent instabilities and reduce turbulence as is done with momentum injection. Understanding the origin of this rotation is also an interesting physics question. This has driven several experimental [6–10], numerical [11–13] and theoretical [14–17] studies. So far, numerical results for intrinsic rotation have only been obtained using global gyrokinetic simulations that have been recently proven to be flawed for radial momentum transport in the core of tokamaks [18].

In this Letter, we use very simple theoretical arguments to show that the velocity difference within the core of a tokamak must scale proportionally to the ion temperature divided by the plasma current. The constant of proportionality is independent of machine size and is of order $c^2/e = 10 \, \mathrm{km} \cdot \mathrm{s}^{-1} \cdot \mathrm{MA} \cdot \mathrm{keV}^{-1}$, where c is the speed of light and e is the proton charge. We show that pulses with hollow intrinsic rotation (counter-current rotation at the magnetic axis and co-current at the edge) from machines whose sizes range from tens of centimeters to several meters, that have very different plasma currents (from 0.1 MA to 2.5 MA), and that are heated by different mechanisms (JET [10], DIII-D [9], TCABR [19] and TCV [7]) follow the theoretical scaling.

Theoretical arguments. In a tokamak plasma, turbulence and collisions transport momentum across magnetic surfaces. Momentum can be injected with neutral beams and radio frequency waves (RF) [20], but in many occasions there is no external source of momentum. When the latter is the case, the toroidal angular momentum flux Π through every flux surface must be zero, even though significant rotation can often be observed experimentally. Only the angular momentum in the toroidal direction is relevant. In the poloidal direction, the flow is strongly damped by collisional processes, which pass the momentum through the magnets to the structure of the tokamak. Thus, to calculate intrinsic rotation profiles, it is necessary to calculate the dependence of Π on the toroidal rotation frequency Ω_ϕ and then solve the equation $\Pi(\Omega_\phi) = 0$ for Ω_ϕ.

Both turbulence and collisions occur on time scales that are longer than the inverse of the gyrofrequency, which means that the particle trajectories can be understood as a fast gyromotion around guiding centers, which move fast along magnetic field lines and drift slowly across them. This is the physical idea underlying gyrokinetics, which is the most commonly used approximation in transport simulations [21–25].

Even in the absence of turbulence and collisions, particles move out of the surface of constant magnetic flux where they started due to the ∇B and curvature drifts, but they remain within a given distance of it. This distance is of the order of the poloidal gyroradius $\rho_\theta = mcv_{th}/eB_\theta$, where e and m are the charge and mass of the particle, v_{th} is the thermal speed, and B_θ is the poloidal component of the magnetic field. Note that $\rho_\theta = (B/B_\theta)\rho$, where ρ is the particle gyroradius and B is the total magnetic field. In most tokamaks, B/B_θ is of order 10. Tokamaks are constructed so that $\rho_\theta \ll L_T$, where L_T is the characteristic length of variation of the temperature T, which we use as our length of reference.

Collisions cause transport, known as neoclassical transport [26], because each collision makes the particle move from one drift orbit to another separated by ρ_θ. Turbulent transport is caused by electromagnetic fluctuations, of which the most virulent are believed to be driven by the ion temperature gradient (ITG). For ITG turbulence well above marginality, the characteristic correlation length is $(B/B_\theta)(a/L_T)\rho \sim \rho_\theta$, where a is the minor radius of the tokamak ($L_T \sim a$). This scaling is not based on the drift orbits as is in the case of collisional transport, but on critical balance between the parallel and the perpendicular dynamics [27]. It is observed in experiments that the turbulent transport scales approximately linearly with B/B_θ [28], as predicted by critical balance [27]

In general, tokamaks are geometrically up-down symmetric to a great degree in the core. In such tokamaks, to lowest order in ρ_θ/L_T, the transport of momentum can only be different from zero if a preferred direction is given by either rotation or rotational shear. The lowest order cancellation of the radial momentum flux in the absence of rotation is due to a fundamental symmetry of the turbulence and the particle motion [29–31]. Here we are assuming $\Omega_\phi \sim v_{th}/R$, this being the ordering for which the rotation and its shear enter in the lowest order gyrokinetic equation [32, 33]. Thus, schematically, to lowest order in ρ_θ/L_T,

$$\Pi \sim -\nu_{\rm t} R^2 \left(\frac{\partial \Omega_\phi}{\partial r} + \frac{\Omega_\phi}{\ell_{\rm pinch}} \right) - \nu_{\rm c} R^2 \frac{\partial \Omega_\phi}{\partial r}, \qquad (1)$$

where r is the radial coordinate, R is the major radius, $\nu_{\rm t}$ is the turbulent viscosity, $-\nu_{\rm t}/\ell_{\rm pinch}$ is the turbulent pinch of momentum [34, 35], and $\nu_{\rm c}$ is the collisional viscosity. Equation (1) has the main features of momentum transport in up-down symmetric tokamaks: momentum transport can only happen when $\Omega_\phi \neq 0$ or $\partial \Omega_\phi/\partial r \neq 0$, and it changes sign when Ω_ϕ and $\partial \Omega_\phi/\partial r$ do [31]. It can be thought of as a Taylor expansion of the complicated function $\Pi(\partial \Omega_\phi/\partial r, \Omega_\phi)$ around $\Omega_\phi = 0$ and $\partial \Omega_\phi/\partial r = 0$.

The equation for intrinsic rotation is $\Pi = 0$, and with the lowest-order expression (1) for Π, the solution is $\Omega_\phi \propto \exp[-\int dr\, \ell_{\rm pinch}^{-1}(1 + \nu_{\rm c}/\nu_{\rm t})^{-1}]$. It is then possible to obtain intrinsic rotation if rotation is generated in
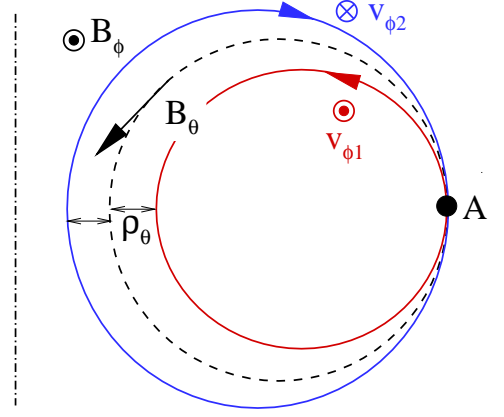

FIG. 1: Sketch of drift orbits.

some region of the plasma (for example, in the edge) and pinched to other regions. However, this mechanism is not fully satisfactory because it cannot explain the variety of observed profiles [10]. In particular, Ω_ϕ cannot change sign, contradicting experimental observations (as we will show in the next section). Unfortunately, to lowest order, Eq. (1) is correct and no other mechanism for intrinsic rotation can be obtained.

If the expansion in $\rho_\theta/L_T \ll 1$ is continued to next order, the rotation and its shear are not the only physical factors that provide a preferred direction and can give raise to momentum transport: the pressure and temperature gradients also break the up-down symmetry. Consider the guiding centers of two particles (1 and 2) that at point A at the outboard midplane of a tokamak have velocities in opposite directions, as sketched in Fig. 1. The dashed line represents the cut of a surface of constant magnetic flux through a poloidal plane (the axis of symmetry is the dash-dot line). The poloidal magnetic field B_θ is parallel to the dashed line and points counterclockwise, whereas the toroidal magnetic field B_ϕ points towards the reader. At point A, particle 1 (red orbit) travels counterclockwise, and since to lowest order it follows the magnetic field, its toroidal velocity $v_{\phi 1}$ is pointing towards the reader. Particle 2 (blue orbit) travels in the opposite direction both poloidally and toroidally. Orbits separate from the flux surface a small distance of order ρ_θ. Particle 1 moves towards the center of the tokamak because its poloidal velocity is counterclockwise. Particle 2 drifts outwards. Because of the temperature gradient, the center of the tokamak is hotter, and particles like particle 1 will have more energy, of the order of $(\rho_\theta/L_T)mv_{th}^2$, breaking the symmetry and, in this simplified picture, making the plasma rotate counterclockwise poloidally, and towards the reader toroidally. Fig. 1 shows that whereas the direction of the magnetic field is unimportant, the vector $\mathbf{B} \times \nabla T$ does give a preferred direction at higher order in ρ_θ/L_T parallel to or against

which the plasma will tend to rotate. The mechanism described here does not determine the sense of the toroidal rotation, but it does demonstrate that background gradients break the up-down symmetry and that the effects of this symmetry breaking are of order ρ_θ/L_T. Calculating all these effects is a rather sophisticated analytical task, involving many factors subtler than the simple argument given above [46].

The next-order contributions to momentum transport in $\rho_\theta/L_T \ll 1$ were first calculated in neoclassical theory [36, 37], where they are proportional to radial derivatives of the ion temperature. Models to calculate the next-order contributions to turbulent transport have also been proposed [16, 17]. Near marginality, the turbulence amplitude is small, and the neoclassical corrections to the distribution function of order ρ_θ/L_T due to finite drift orbit size are the dominant mechanism that breaks the up-down symmetry of the turbulence. Well above marginality, the characteristic eddie size is ρ_θ [27], allowing the turbulence to sample regions in which the temperature gradient differs by ρ_θ/L_T, and breaking the symmetry this way. In general, we expect the new next-order terms to depend strongly on density and temperature gradients because these drive the turbulence. Schematically, as shown in [17], we may write

$$\Pi \sim -\nu_t R^2 \left[\frac{\partial \Omega_\phi}{\partial r} + \frac{\Omega_\phi}{\ell_{\text{pinch}}} + O\left(\frac{\rho_\theta}{L_T}\frac{v_{th}}{RL_T}\right) \right]$$
$$-\nu_c R^2 \left[\frac{\partial \Omega_\phi}{\partial r} + O\left(\frac{\rho_\theta}{L_T}\frac{v_{th}}{RL_T}\right) \right]. \quad (2)$$

From (2), setting $\Pi = 0$ and assuming that the scale length of Ω_ϕ is of order L_T, we obtain $R\Omega_\phi \sim (\rho_\theta/L_T)v_{th} \sim (c/eB_\theta)(T/L_T)$, where $T = mv_{th}^2/2$ is the temperature. The poloidal magnetic field is given by the toroidal plasma current I_p, $B_\theta \sim I_p/cL_B$, where L_B is the characteristic length of variation of B_θ. Therefore, $R\Omega_\phi \sim (L_B/L_T)(c^2/e)(T/I_p)$. In the core, L_B and L_T are both of the order of the minor radius a, so the toroidal velocity is

$$V_\phi = R\Omega_\phi \sim \frac{c^2}{e}\frac{T}{I_p}. \quad (3)$$

This equation gives the scaling of intrinsic rotation in the core with temperature and plasma current. It is *independent of machine size.* The dimensional constant of proportionality is $c^2/e = 10\,\text{km}\cdot\text{s}^{-1}\cdot\text{MA}\cdot\text{keV}^{-1}$.

Experimental measurements. We now compare experimental data from different machines that show similarities in their intrinsic rotation profiles. In Fig. 2 two pulses from JET represent two distinct types of intrinsic rotation profiles: the ones in which the toroidal velocity increases from the magnetic axis towards the edge of the tokamak (red profile), which we call *hollow profiles*, and the ones in which it decreases (blue profile), which we call
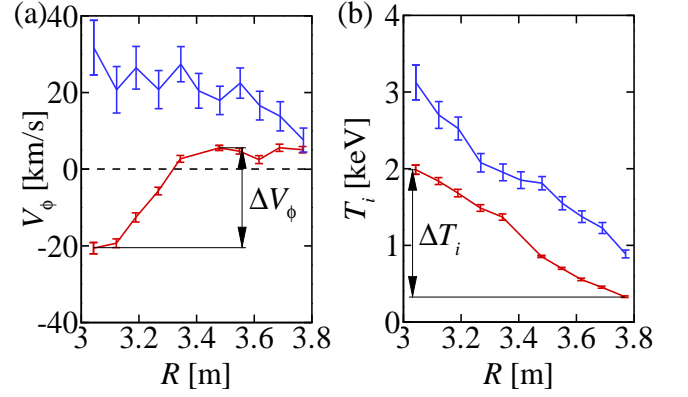

FIG. 2: Intrinsic rotation profiles (a) and ion temperature profiles (b) in JET plasmas with ICRH, pulses 66395 (red) and 74692 (blue). The rotation in the co-current direction is positive rotation. The position of the magnetic axis is around $R = 3\,\text{m}$, the separatrix is around $R = 3.8\,\text{m}$.

peaked profiles (the toroidal velocity is deemed positive if it is co-current). The two pulses in Fig. 2 have very different input power and plasma current, and they are only meant to be examples of the two types of velocity profiles. The peaked profiles need not have higher temperature gradients than the hollow profiles. The velocity at the edge is mostly co-current, and this seems to be common to all tokamaks with low magnetic ripple in the absence of momentum injection. In JET, the hollow profiles correspond to Ohmic shots and some of the Ion Cyclotron Resonance Heating (ICRH) pulses in both Low-Confinement Mode (L-mode) [10] and High-Confinement Mode (H-mode) [38]. The cases with peaked profiles are all ICRH L-mode and H-mode shots.

To check (3), we compare the pulses with hollow core velocity profile for four different tokamaks: JET [10], DIII-D [9], TCABR [19] and TCV [7]. To characterize the velocity generated intrinsically in the core, we use the difference in toroidal velocity ΔV_ϕ between the minimum of toroidal velocity closest to the magnetic axis on the outboard side and the first maximum encountered when moving from the magnetic axis towards the edge on the outboard side. This definition of ΔV_ϕ is illustrated in Fig. 2(a). The parameter ΔV_ϕ attempts to exclude any intrinsic velocity generated at the edge – most likely by means not covered in our theoretical discussion above. To give a measure of the sources generating intrinsic rotation in (2), we use the difference in ion temperature ΔT_i between the magnetic axis and the temperature at the top of the pedestal in H-modes, or the temperature measurement that is the closest to the separatrix in L-modes. The difference ΔT_i, illustrated in Fig. 2(b), excludes the ion temperature jump in the pedestal in the case of H-modes. Fig. 3 shows $I_p \Delta V_\phi$ vs. ΔT_i for various tokamaks
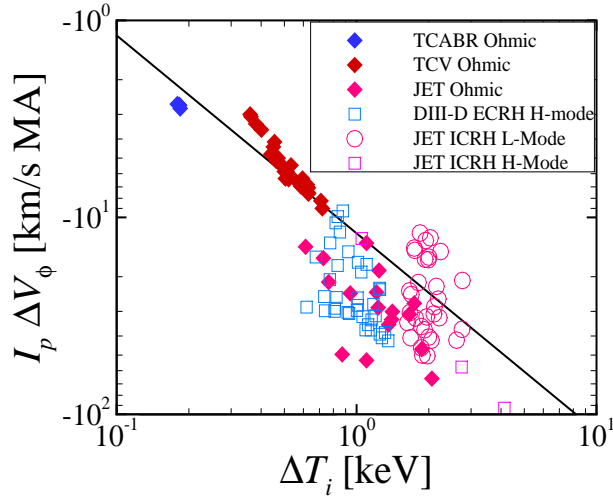
FIG. 3: Toroidal velocity difference in the core ΔV_ϕ multiplied by plasma current I_p against the ion temperature difference ΔT_i in the plasma core. The line is the least-square fit of the data to (4). The slope is $18\,\mathrm{km}\cdot\mathrm{s}^{-1}\cdot\mathrm{MA}\cdot\mathrm{keV}^{-1}$.

[47]. According to (3), we expect

$$I_p\Delta V_\phi = \alpha\frac{c^2}{e}\Delta T_i. \qquad (4)$$

The dimensionless prefactor α could not be determined in our qualitative theoretical discussion, but we can find its value from the present experimental analysis. The data is consistent with an approximate linear dependence with a slope of $(18\pm4)\,\mathrm{km}\cdot\mathrm{s}^{-1}\cdot\mathrm{MA}\cdot\mathrm{keV}^{-1}$ for all machines, giving $\alpha\simeq1.8\pm0.4$. The slope was determined by least-square fitting and the error is the 99% confidence interval. In Fig. 3 there are Ohmic, ICRH and Electron Cyclotron Resonance Heating (ECRH) shots, L- and H-modes, plasma currents spanning from 0.1 MA to 2.5 MA, and machines of sizes ranging from tens of centimeters (TCABR) to meters (JET). The fact that both the scaling and the prefactor seem to be valid for this variety of situations suggests that the theoretical ideas proposed above are robust.

When the same analysis was attempted for the peaked profiles in JET, the trend was not so clear, but we cannot conclude that the scaling is absent either. The study of peaked profiles will be the object of a future publication. Here we review several possible explanations for the lack of a clear scaling. In [8, 12] a change from Trapped Electron Mode (TEM) driven turbulence to ITG turbulence was proposed as the cause for the transition between peaked and hollow profiles. If this is the case, ΔT_i is not a good parameter to work with because TEM turbulence depends strongly on the electron density gradient, for which ΔT_i is not a good proxy, and on the electron temperature profile that for low collisionality may differ from T_i. It is also possible that the peaked-profile cases

are dominated by the inward pinch of momentum generated at the edge [10], making the rotation in the core correlated to the parameters at the edge and not to the parameters of the core. With our preliminary analysis of peaked profiles in JET, we cannot decide if the transition from hollow to peaked profiles is due to the reasons given above, or other reasons not considered here. Experiments in DIII-D show that shaping affects intrinsic rotation, with high triangularity shots tending to have peaked profiles. Shaping may affect ITG and TEM turbulence differently, making one or the other type of turbulence dominant for high triangularity and hence deciding the direction of rotation in this way, or it may have an effect on the direction in which ITG or TEM turbulence pushes the plasma. Further study is needed. Even though the trend with ΔT_i and I_p was not so clear, the velocity difference ΔV_ϕ was still of the same order as (3).

Discussion. Using simple theoretical arguments, we have shown that the intrinsic rotation generated in the core must scale according to (4). Hollow intrinsic rotation profiles from very different tokamaks follow this scaling. The scatter in Fig. 3 is to be expected since (4) is derived from an order of magnitude estimate and prefactors of order unity may vary from shot to shot.

There are ways of generating intrinsic rotation that have not been considered in this Letter. For example, in the core, RF heating can transport momentum [39, 40] due to the large orbits of energetic ions. In the edge, direct particle losses can generate rotation [41]. It seems that these effects are not important in the cases presented in Fig. 3 because these include shots with and without energetic ions, and with and without a pedestal. We do not know how generic this is. We have introduced a dimensionless parameter $\alpha = eI_p\Delta V_\phi/c^2\Delta T_i$, which was of order unity for a variety of regimes and machines considered here. It would be very instructive to quantify experimentally measured rotation in other cases in terms of this parameter. In cases that α is significantly larger than unity, the rotation must have external origin, such as energetic ions, edge effects or momentum injection.

The experimental results presented above cannot determine if the transport of momentum is dominated by collisions or turbulence because both have the same scaling (3). Since turbulent viscosity is of the same order as the thermal diffusivity [35, 42–44], and turbulent transport usually dominates, we expect the ρ_θ/L_T corrections to the turbulent momentum transport to play the dominant role in driving intrinsic rotation.

* Electronic address: fparra@mit.edu

[1] P. C. de Vries et al., Plasma Phys. Control. Fusion **38**, 467 (1996).
[2] J. W. Connor et al., Nucl. Fusion **44**, R1 (2004).
[3] P. C. de Vries et al., Nucl. Fusion **49**, 075007 (2009).
[4] P. Mantica et al., Phys. Rev. Lett. **102**, 175002 (2009).
[5] K. Ikeda et al., Nucl. Fusion **47**, E01 (2007).
[6] J. E. Rice et al., Nucl. Fusion **47**, 1618 (2007).
[7] A. Scarabosio et al., Plasma Phys. Control. Fusion **48**, 663 (2006).
[8] B. P. Duval et al., Plasma Phys. Control. Fusion **49**, B195 (2007).
[9] J. S. deGrassie et al., Phys. Plasmas **14**, 056115 (2007).
[10] L.-G. Eriksson et al., Plasma Phys. Control. Fusion **51**, 044008 (2009).
[11] W. X. Wang et al., Phys. Plasmas **17**, 072511 (2010).
[12] Y. Camenen et al., Nucl. Fusion **51**, 073039 (2011).
[13] W. X. Wang, T. S. Hahm, S. Ethier, L. E. Zakharov and P. H. Diamond, Phys. Rev. Lett. **106**, 085001 (2011).
[14] P. H. Diamond et al., Phys. Plasmas **15**, 012303 (2008).
[15] Y. Camenen et al., Phys. Rev. Lett. **102**, 125001 (2009).
[16] F. I. Parra and P. J. Catto, Plasma Phys. Control. Fusion **52**, 045004 (2010).
[17] F. I. Parra, M. Barnes and P. J. Catto, Nucl. Fusion **51**, 113001 (2011).
[18] F. I. Parra and P. J. Catto, Phys. Plasmas **17**, 056106 (2010).
[19] J. H. F. Severo et al., Nucl. Fusion **43**, 1047 (2003).
[20] A. Ince-Cushman et al., Phys. Rev. Lett. **102**, 035002 (2009).
[21] W. Dorland, F. Jenko, M. Kotschenreuther and B. N. Rogers, Phys. Rev. Lett. **85**, 5579 (2000).
[22] J. Candy and R. E. Waltz, J. Comput. Phys. **186**, 545 (2003).
[23] T. Dannert and F. Jenko, Phys. Plasmas **12**, 072309 (2005).
[24] A. G. Peeters et al., Comput. Phys. Comm. **180**, 2650 (2009).
[25] M. Barnes et al., Phys. Plasmas **17**, 056109 (2010).
[26] F. L. Hinton and R. D. Hazeltine, Rev. Mod. Phys. **48**, 239 (1976).
[27] M. Barnes, F. I. Parra and A. A. Schekochihin, Phys. Rev. Lett. **107**, 115003 (2011).
[28] C. C. Petty, J. E. Kinsey and T. C. Luce, Phys. Plasmas **11**, 1011 (2004).
[29] A. G. Peeters and C. Angioni, Phys. Plasmas **12**, 072515 (2005).
[30] H. Sugama et al., Plasma Phys. Control. Fusion **53**, 024004 (2011).
[31] F. I. Parra, M. Barnes and A. G. Peeters, Phys. Plasmas **18**, 062501 (2011).
[32] M. Artun and W. M. Tang, Phys. Plasmas **1**, 2682 (1994).
[33] H. Sugama and W. Horton, Phys. Plasmas **5**, 2560 (1998).
[34] A. G. Peeters, C. Angioni and D. Strintzi, Phys. Rev. Lett. **98**, 265003 (2007).
[35] G. Tardini et al., Nucl. Fusion **49**, 085010 (2009).
[36] P. J. Catto and A. N. Simakov, Phys. Plasmas **12**, 012501 (2005).
[37] S. K. Wong and V. S. Chan, Phys. Plasmas **16**, 122507 (2009).
[38] M. F. F. Nave et al., submitted to Plasma Phys. Control. Fusion (2011).
[39] F. W. Perkins et al., Phys. Plasmas **8**, 2181 (2001).
[40] L.-G. Eriksson and F. Porcelli, Nucl. Fusion **42**, 959 (2002).
[41] J. S. deGrassie et al., Nucl. Fusion **49**, 085020 (2009).
[42] F. J. Casson et al., Phys. Plasmas **16**, 092303 (2009).
[43] M. Barnes et al., Phys. Rev. Lett. **106**, 175004 (2011).
[44] E. G. Highcock et al., Phys. Rev. Lett. **105**, 215003 (2010).
[45] E. G. Highcock et al., Phys. Plasmas **18**, 102304 (2011).
[46] To give an idea of the complexity of the theoretical problem, we point out that the poloidal velocity will not be counterclockwise at low collisionality, as suggested by Fig. 1, but clockwise due to the collisional friction between particles of the type sketched in Fig. 1 and a population of trapped particles [26]. Determining the toroidal rotation requires even more work than the poloidal velocity, and the finite-orbit-width effects come in through other mechanisms. For example, the poloidal velocity breaks the up-down symmetry and gives a preferred direction to the turbulent and collisional transport of toroidal angular momentum.
[47] The data for TCV was obtained from [7]. In that article, the authors plotted the velocity at the magnetic axis multiplied by I_p against the temperature at the magnetic axis. This is approximately the same as $I_p \Delta V_\phi$ vs. ΔT_i because both the rotation and the temperature at the edge are small compared to their values at the magnetic axis.